Springer

KSME

Journal of Mechanical Science and Technology 26 (9) (2012) 2985~2994
www.springerlink.com/content/1738-494x
DOI 10.1007/s12206-012-0705-z

Effect of channel and plenum aspect ratios on the performance of microchannel heat sink under different flow arrangements †

S. S. Sehgal[1], Krishnan Murugesan[2,*] and S. K. Mohapatra[3]

[1]*Department of Mechanical & Automotive Engineering, Swift Institute of Engineering & Technology, Punjab, India*
[2]*Department of Mechanical & Industrial Engineering, Indian Institute of Technology, Roorkee, India*
[3]*Department of Mechanical Engineering, Thapar University, Punjab, India*

(Manuscript Received November 10, 2011; Revised April 5, 2012; Accepted April 30, 2012)

Abstract

Microchannels based heat sinks are considered as potential thermal management solution for electronic devices. The overall thermal performance of a microchannel heat sink depends on the flow characteristics within microchannels as well as within the inlet and outlet plenum and these flow phenomena are influenced by channel aspect ratio, plenum aspect ratio and flow arrangements at the inlet and outlet plenums. In the present research work an experimental investigation has been carried out to understand how the heat transfer and pressure drop attributes vary with different plenum aspect ratio and channel aspect ratio under different flow arrangements. For this purpose microchannel test pieces with two channel aspect ratios, 4.72 and 7.57 and three plenum aspect ratios, 2.5, 3.0 and 3.75 have been tested under three flow arrangements, namely U-, S- and P-types. Test runs were performed by maintaining three constant heat inputs, 125 W, 225 W and 375 W in the range $224.3 \leq R_e \leq 1121.7$. Reduction in channel width (increase in aspect ratio, defined as depth to width of channel) in the present case has shown about 126 to 165% increase in Nusselt number, whereas increase in plenum length (reduction in plenum aspect ratio defined as width to length of plenum) has resulted in 18 to 26% increase in Nusselt number.

Keywords: Channel aspect ratio; Flow arrangements; Microchannel heat sink; Nusselt number; Plenum aspect ratio; Pressure drop

1. Introduction

The past couple of decades has witnessed a rapid progress in the applications of Integrated Circuits (ICs) forcing the size of these circuits to decrease drastically with high demand on increased operating speeds and package densities. These factors have lead to high die temperatures which are detrimental to circuit performance and reliability. Hence there is a need for new and innovative technologies for the development of embedded cooling solutions, IC-level integration of thermal sensors and heat sinks, and systematic synthesis techniques for ICs that contain embedded heat dissipation mechanisms. Microchannels and minichannels based heat sinks are the obvious choice as they provide large heat transfer surface area per unit volume of fluid flow and generally these microchannel heat sink use liquids as coolants. The large surface to volume ratio gives rise to high rate of heat transfer, making these heat sink devices as excellent and compact cooling systems. Tuckerman and Pease [1] started their pioneer experimental work to examine the suitability of high-performance heat sinks for cooling of very large-scale integration (VLSI) systems. Most of the research works on microchannel heat sinks (MCHS) have focused on the study of heat transfer and fluid flow distribution within the microchannels. However, very limited research works are available to understand the effect of flow arrangements and size of the inlet and outlet plenums on the performance of MCHS. Various numerical and experimental studies [2] show that heat transfer and fluid flow behavior within mini and micro channel devices are influenced by the geometry, aspect ratio and flow arrangements of the heat sinks.

Chein and Chen [3] numerically analyzed the fluid flow and heat transfer in MCHSs by solving 3D governing equations for both fluid flow and heat transfer analysis using finite volume scheme. Their computational domain consisted of the entire heat sink, including the inlet/outlet ports, inlet/outlet plenums, and microchannels. They observed that the resultant flow field and temperature distributions inside the heat sink varied significantly for a given pressure drop on account of the difference at inlet/outlet flow arrangements. For all of the heat sinks investigated (U-, V-, I-, N-, D-, and S-types), the highest heat sink temperature was observed at the edge of the heat sink. This was attributed to the absence of heat dissipation by fluid convection. They found that the V-type heat sink has the best performance among the heat sinks studied. For the heat sinks with horizontal fluid supply and collection, i.e., the I-,

*Corresponding author. Tel.: +91 1332 285635, Fax.: +91 1332 285665
E-mail address: krimufme@iitr.ac.in
† Recommended by Associate Editor Man-Yeong Ha

N-, D-, and S-type heat sinks, they observed velocity mal-distribution to be responsible for greater degradation of performance compared to the heat sinks with vertical fluid supply and collection, i.e., the U and V-type heat sinks. They, however, neither explained the term velocity mal-distribution in detail nor quantified it. Lee and Garimella [4] developed three-dimensional numerical simulations for thermally developing laminar flow in microchannels of different aspect ratios ranging from 1 to 10. Based on their results on temperature and heat flux distributions, they studied the variation of both the local and average Nusselt numbers as a function of dimensionless axial distance and the channel aspect ratio. They also proposed generalized correlations for both the local and average Nusselt numbers in the thermal entrance region. Simon Jayaraj et al. [5] presented a review on microchannel fluid flow and mixing. Their work includes the physics of flow in microchannels and integrated simulation of microchannel flow, control models of flow, and electro-kinetically driven microchannel flow. They have presented a survey of important numerical methods which are currently popular for microchannel flow analysis and different options for flow mixing in microchannels.

Recently, Sehgal et al. [6] studied experimentally the effect of entrance and exit conditions that prevail due to varying flow arrangements, U-, S- and P-type, on the thermal performance of MCHS. They reported that for a constant Reynolds number, the maximum heat transfer was noticed for the U-type flow arrangement followed by P-type and S-type and maximum pressure drop was observed for S-type flow arrangement followed by U-type and P-type. Researchers have studied the effect of inlet and exit plenums on thermal performance of MCHS but till date, no detailed experimental study has been reported in the literature to understand the influence of inlet and exit plenums on convective heat transfer within the MCHS.

In the present work, an attempt is made to study the effect of inlet/outlet plenum aspect ratio along with channel aspect ratio on heat transfer and pressure drop characteristics of MCHS. A detailed experimental examination has been carried out using microchannel test pieces with two channel aspect ratios and three plenum aspect ratios. These tests have been conducted for three flow arrangements, namely U-, S- and P-types at different heat inputs for varying Reynolds numbers in laminar flow region.

2. Experimental procedure

2.1 Microchannel test set up

The schematic diagram of the experimental test set-up is shown in Fig. 1. Deionised water was pumped (Make: Micropump, Series 200) from the liquid reservoir to the test section, through a 15 μm filter. The outlet fluid from the MCHS was cooled by forced convective heat exchanger (Make: Thermaltake; Model: TMG1) and returned to the liquid reservoir, thus forming a closed loop. The inlet and outlet fluid temperatures

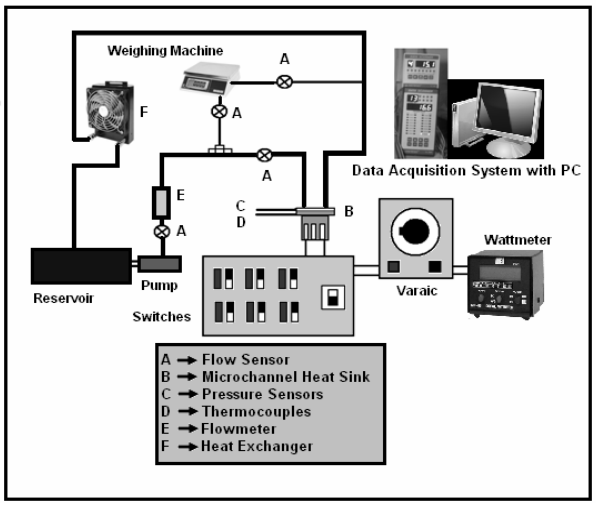

Fig. 1. Schematic layout of experimental setup.

were measured using precision T-type thermocouples (Make: Omega; Model: HYP1-30-1/2-T-G-60-SMPW-M). A needle valve fitted on the flow meter (Make: EGE; Model: SDN 552; Working range: 0.01-10 L/min; Precision: 2%) downstream of the pump allows fine adjustment of flow rate to obtain Reynolds number range of 224.3–1121.7. All the temperature readings were collected by a high speed data acquisition system (Make: Ambetronics; Model: TC-1600F panel mounted), attached to a computer. Fig. 2(a) shows the actual dimensions of the MCHS. In this work the aspect ratio for channel (AR_c) and plenum (AR_p) are defined as:

$$AR_c = \frac{\text{microchannel depth}}{\text{microchannel width}} \quad \text{and} \quad AR_p = \frac{\text{plenum width}}{\text{plenum length}}$$

There are 20 arrays of parallel microchannels in the MCHS, each having 530 μm or 330 μm width with a constant depth of 2.5 mm giving AR_c of 4.72 and 7.57 respectively. The inlet and outlet plenums have constant width of 30 mm and depth 2.5 mm. Their length was varied as 12, 10 and 8 mm to have AR_p of 2.5, 3.0 and 3.75 respectively.

2.2 Pressure and temperature measurement

Pressure transducers (Make: KELLER Druckmesstechnik; Series 33X) were fixed at the two adapter locations (Fig. 2(a), 3) for measuring the total pressure drop for the MCHS. Each pressure transducer has an accuracy of ±0.1% and resolution of 0.002% over the standard pressure range 0–3 bar and they were calibrated using a standard dead weight tester. For the temperature measurement, T-type thermocouples were inserted at twenty locations both at the inlet and outlet plenums of the MCHS (Fig. 2(a)) at an equal distance of 5±0.01 mm. The data obtained were used to study the temperature distribution within the plenums. Two additional thermocouples of the same type were fixed at the adapter locations for measuring

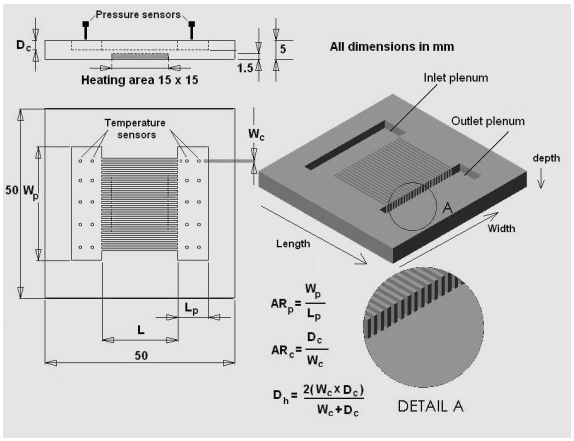

(a)

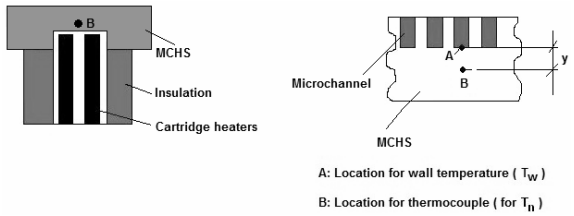

(b)

Fig. 2. (a) Test piece with dimensions; (b) Arrangement for wall temperature measurement (Not to scale).

fluid temperatures at the entry and exit of the MCHS. The error associated with the thermocouple measurements was estimated as less than 2%. Thermocouples were calibrated by Universal Dry Block Temperature Calibrator (Make: Nagman; Model MTC 350). The heat input to the MCHS was supplied using electric operated cartridge heaters (Make: BEECO) of range 100 – 800 W. The measurement uncertainty associated with the Wattmeter (Make: MFJ; Model: 826) was less than 0.8%. The data acquisition system has an accuracy of ±0.25% FS and resolution of 0.001% FS.

2.3 Flow arrangements

One of the important objectives of the present research is to analyze the variation of convective heat transfer within the MCHS due to the use of different flow arrangements at the inlet and outlet plenums. In the present research work, three different types of flow arrangements (Fig. 3) namely P-type, U-type and S-type have been studied, where P stands for the perpendicular, U stands for U-shape and S stands for serpent shape. In order to achieve these flow entries and exits of water to and from the plenum, suitable piping arrangements were employed.

2.4 Heat transfer calculation

The overall performance of the MCHS is estimated in terms of convective heat transfer along with the pressure drop. The

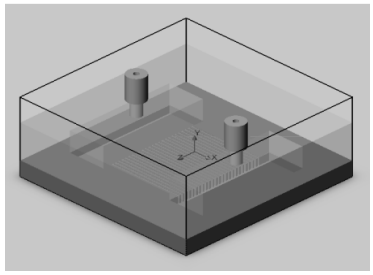

(a) P-type

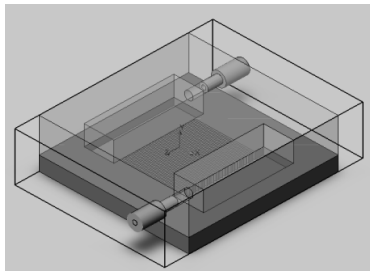

(b) S-type

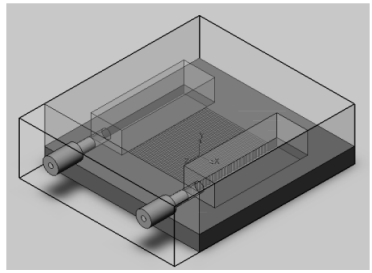

(c) U-type

Fig. 3. Different types of flow arrangements.

pressure drop parameter is important from operating cost point of view. The actual heat input to the heat sink is supplied through the cartridge heaters provided at the bottom section of the heat sink. Lee et al. [7] suggests 85–90% of power provided to the cartridge heaters was transferred to water. In the present work, in order to obtain a desired heating load to be carried away by the water, the power input to the cartridge heaters was adjusted. In the absence of viscous dissipation effects, for steady flow through the microchannels, the actual heat convected from the inside surface of the channels to the fluid stream can be equated to the sensible heat carried away by the fluid as

$$q = \dot{m} C_p \left(T_o - T_i \right) \tag{1}$$

where $\dot{m} = \rho \times Q$

The fluid temperatures T_i and T_o, are measured by the thermocouples located at the entry and exit adapters of the MCHS and the average of these temperatures is taken as the mean fluid temperature, T_m. The density, ρ and specific heat capacity, C_p is calculated based on the mean fluid temperature T_m. The volumetric flow rate Q is measured with a flow meter

calibrated using a digital weighing scale [6]. For internal flows, the convective heat transfer from the walls of the channels to the fluid stream is calculated from Newton's law of cooling as

$$q = hAN(T_w - T_m) \tag{2}$$

where h is the convective heat transfer coefficient, A is the surface area available for heat transfer per channel ($L(W_c + 2D_c)$), N is the total number of microchannels and T_w is the temperature of the channel wall.

As it is difficult to measure the wall temperature of the microchannels directly, it is computed by assuming one-dimensional heat conduction. For this purpose, the temperature closer to the bottom wall of the channel, (T_n) is measured as shown in Fig. 2(b). Assuming that all the sensible heat gained by the water in the microchannel heat sink is equal to the heat conducted through the wall, we can write the heat conducted as

$$q = k_{cu} A_h \frac{(T_n - T_w)}{y} \tag{3}$$

in which k_{cu} is the thermal conductivity of the material of the heat sink, A_h is the MCHS bottom heated area (Fig. 2(a)) over which heating is provided by the cartridge heater, y is the distance between the bottom wall of the channel and the point at which thermocouple is embedded to measure T_n (Fig. 2(b)). For microchannels made of copper with dimensions considered in the present work, the temperature gradient along the length and width of the channels is assumed to be very small and hence it is neglected. The wall temperature of the channel, T_w is computed from Eq. (3). However, the mean fluid temperature T_m increases along the length of the channel as the channel wall temperature becomes higher than the mean fluid temperature. For constant uniform surface wall heat flux condition, such as the one considered in the present research, the variation of T_m with the length of the channel is assumed to be linear on a similar ground as considered by Lee et al. [7].

The fluid temperature at the inlet and outlet plenums are measured from the twenty thermocouples positioned (Fig. 2(a)) within the MCHS. It was also assumed that the temperature at any location within the microchannel can be computed from the heat balance equation:

$$T_m - T_{mi} = \frac{q}{\dot{m} C_p} \frac{x}{L} \tag{4}$$

where T_{mi} is the fluid temperature at the inlet plenum obtained as the average of the temperatures measured using the thermocouples.

After estimating T_w and T_m, the convective heat transfer coefficient can be computed from Eq. (2). Nusselt number is the heat transfer characteristics that represents the convective heat transfer performance of a MCHS and is defined as follows:

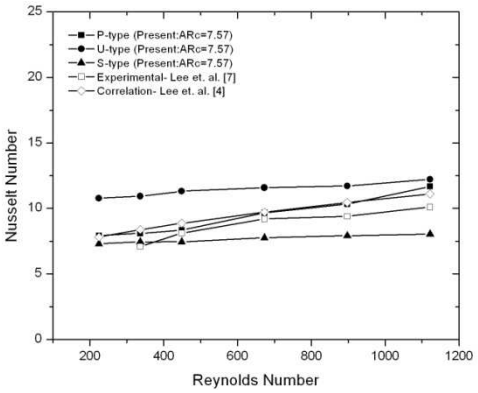

Fig. 4. Validation results for Nusselt number [6].

$$Nu = \frac{hD_h}{k} \tag{5}$$

where D_h is the hydraulic diameter defined as

$$D_h = \frac{2(W_c \times D_c)}{W_c + D_c} \tag{6}$$

where W_c and D_c are width and depth of a microchannel, k is the thermal conductivity of fluid evaluated at the mean fluid temperature, T_m and h is the heat transfer coefficient that can be evaluated using Eq. (2). The flow Reynolds number is defined as

$$R_e = \frac{\rho V_f D_h}{\mu} \tag{7}$$

where V_f is the inlet fluid velocity [6] computed as

$$V_f = \frac{Q}{N \times A_c} \tag{8}$$

where $A_c = W_c \times D_c$.

Once the system attained steady state conditions, readings from flow meter, thermocouples, pressure transducers and Wattmeter were recorded and the Nusselt and Reynolds number were computed using Eqs. (5)-(8).

3. Results and discussions

3.1 Validation of experimental procedure

For the purpose of validating the experimental set up and procedure, initial test runs were carried out in the MCHS experimental set up for P-, U- and S-type flow arrangements for six Reynolds number at a power input of 225 W with AR_c = 7.57 and AR_p = 3. The variation of Nusselt number with Reynolds number was compared with the results published by Lee et al. [7] as shown in Fig. 4. The comparison shown in the figure indicates that our experimental results are in close

agreement with the results reported in the above reference. After the validation test runs, the experiments were planned for the present work according to the following test matrix.

3.2 Test matrix

In order to evaluate the thermal performance of the MCHS the test matrix was made with three flow arrangements, P-, U- and S-types; three heat input values, 125 W, 225 W and 375 W; six Reynolds numbers, 224.3, 336.5, 448.7, 673.0, 897.4 and 1121.7; three inlet and outlet plenum aspect ratios 2.5, 3.0 and 3.75, and two channel aspect ratios 4.72 and 7.57 giving rise to a total of 324 experimental trial runs.

3.3 Thermal performance of MCHS

The thermal performance of microchannel heat sink is analyzed by computing the variation of Nusselt number with Reynolds number for various test cases. The effect of channel aspect ratio, plenum aspect ratio and flow arrangements at different heat input values on Nusselt number is discussed in detail in the following sections.

3.3.1 Effect of channel aspect ratio and plenum aspect ratio

Two different channel aspect ratios are obtained by varying the channel width to 330 μm and 530 μm, keeping the channel depth constant, giving rise to AR_c = 7.57 and 4.72 respectively. Similarly, three plenum aspect ratios 3.75, 3 and 2.5 are obtained by varying plenum length to 8 mm, 10 mm and 12 mm respectively keeping the width constant at 30 mm. Nusselt number variation results are presented for three heat input values in Figs. 5 to 7, wherein in each figure results are given for two channel aspect ratios and for a given channel aspect ratio: nine plots are shown for the combinations of three flow arrangements at three plenum aspect ratios. In these figures the symbols denote different flow arrangements, P-, U- and S-types, whereas the different line styles indicate different plenum aspect ratios. The variation of Reynolds number from 224.3 to 1121.7 is obtained by varying the fluid velocity from 0.26 to 1.28 m/s for AR_c = 4.72. With increase in fluid velocity the fluid momentum transport in the axial direction increases, resulting in thinning of boundary layer and this enhances convective heat transfer. As the channel wall receives heat continuously from the cartridge heater, the fluid momentum is also accompanied by the bulk transport of heat from the wall towards the full extent of the fluid stream, thus raising the mean temperature of the fluid stream. Hence increase in fluid velocity gives rise to increase in convective heat transfer, resulting in increase in Nusselt number as seen from Fig. 5(a). This trend is observed for all the three flow arrangements at different plenum aspect ratios. However, with regard to the flow arrangement, U-type always records a higher Nusselt number followed by P- and S-types. It is seen from the above figure that as the plenum aspect ratio is increased from 2.5 to 3.75, the Nusselt number decreases for all the Reynolds numbers. The maximum Nusselt number is obtained for AR_p = 2.5

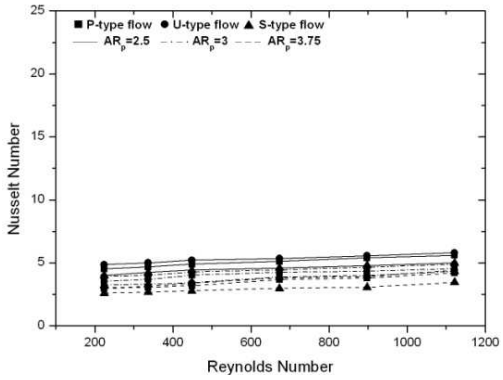

(a) AR_c = 4.72

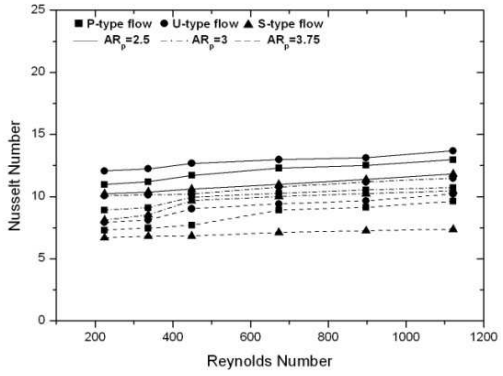

(b) AR_c = 7.57

Fig. 5. Effect of channel aspect ratio on Nusselt number at 125 W heat input.

for U-type flow arrangement followed by P-type and S-type arrangements and the minimum Nusselt number is obtained at AR_p = 3.75 for S-type flow arrangement.

As far as the plenum aspect ratio is concerned the maximum Nusselt number is obtained only at the lowest aspect ratio for a given flow arrangement. This means that for the fixed value of plenum width, when the length of the plenum (Fig. 2(a)) is increased the convective heat transfer is increased. This is because with increase in length of the plenum the flow length of flow regime in the inlet/outlet plenum available for the fluid entering/leaving the channels, increases resulting in enhanced convective heat transfer. It is to be noted that the cooling process that takes place in MCHS is a dynamic process and by the time the fluid enters and comes out of the microchannels the heat should have been absorbed by the liquid. This can take place without interruption only when sufficient length of flow regime is maintained within the inlet/outlet plenum and this is well achieved with increased length of plenum. In addition to this, the increased plenum length will also minimize any entry length phenomena associated with hydrodynamic flow conditions within the channels. These expected phenomena are correctly predicted by the results shown in the above figures.

3.3.2 Flow arrangements

With regard to the flow arrangements, from Fig. 3 one can easily notice that U-type flow arrangement ensures prolonged flow regime in the plenums compared to P-type and S-type flow arrangements. In the P-type flow arrangement as the fluid enters the plenum in the perpendicular direction, it strikes the plenum base directly but this does not ensure perfect fluid distribution within the microchannels. When we look at the S-type flow arrangement, due to its position of outlet just opposite to the inlet position, here again the flow distribution is not fully ensured. However, in the case of U-type flow arrangement the inlet and exit positions of the flow lie on the same side, ensuring longer flow regimes in the inlet/outlet plenum which attributes to the maximum Nusselt number. Fig. 5(b) shows the Nusselt number variation for the channel aspect ratio, 7.57. The trend is almost very similar to the one observed for the channel aspect ratio, 4.72, except another considerable variation observed at lower Reynolds numbers for P-type and S-type flow arrangements at AR_p = 3.0 and 3.75. However, with increase in channel aspect ratio, there is a overall increase in Nusselt number for all the cases of flow arrangements and plenum aspect ratios but maintaining the same trend of yielding the maximum Nusselt number at lower value of plenum aspect ratio. The reasons for this can be explained as follows: when the channel aspect ratio is increased, that is for the constant channel depth, the width of the channel is decreased, and the flow distribution within the channels is well streamlined so that the resistance for heat transfer decreases. This decrease in width has resulted in increase in flow velocity from 0.38 m/s to 1.92 m/s corresponding to the six Reynolds numbers considered in the present work. When velocity is increased, the wall shear stress also increases resulting in enhanced fluid momentum transport within the channel width at any given Reynolds number. Hence the bulk heat transport from the channel wall is also increased resulting in increase in Nusselt number with Reynolds number. It can be observed from Fig. 5 that as the channel aspect ratio is increased from 4.72 to 7.57, the Nusselt number value is almost doubled for all the plenum aspect ratios and flow arrangements.

Fig. 6(a) and 6(b) show the Nusselt number variation with Reynolds number for AR_c = 4.72 and 7.57 respectively for a heat input of 225 W. For this case also, the maximum Nusselt number was observed only at AR_p = 2.5 and AR_c = 7.57 for U-type flow arrangement. The increase in Nusselt number almost follows the trend exhibited for the heat input of 125 W. However, the difference in Nusselt number due to the variation in AR_p is more pronounced for AR_c = 7.57 when the heat input was increased from 125 W to 225 W. A similar trend is also observed for change in flow arrangement as well. It is to be noted that the minimum Nusselt number observed at AR_c = 7.57 for S-type flow arrangement is much higher than the maximum Nusselt number obtained at AR_c = 4.72 for U-type flow arrangement. It is clear from these behaviors that the channel aspect ratio plays an important role in deciding the

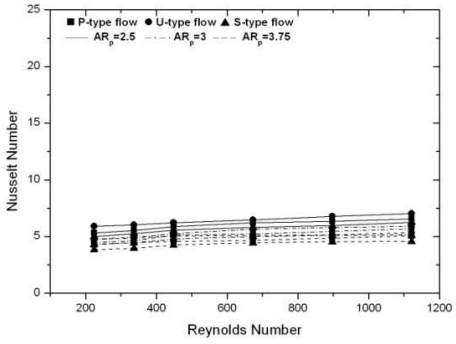

(a) AR_c = 4.72

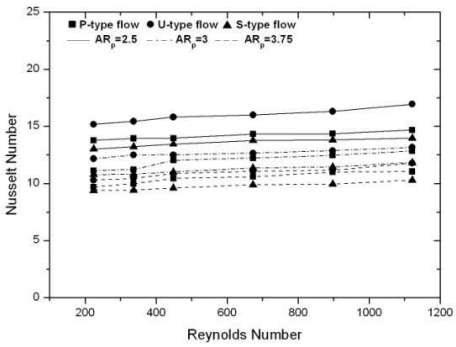

(b) AR_c = 7.57

Fig. 6. Effect of channel aspect ratio on Nusselt number at 225 W heat input.

maximum convective heat transfer at a lower plenum aspect ratio. However, proper combination of channel aspect ratio with plenum aspect ratio and flow arrangement will yield the maximum Nusselt number, making the MCHS compact for a given heat input. Nusselt number results obtained for heat input of 375 W is depicted in Fig. 7(a) and 7(b) for AR_c = 4.72 and 7.57 respectively. The Nusselt number continues to increase with increase in Reynolds number for AR_c = 4.72 as well as for ARc = 7.57. However, a considerable increase is observed for U-type flow arrangement followed by P- and S-types for the lowest plenum aspect ratio. The reason for this behavior may be due to the increased heat potential available for the fluid stream for the same inlet temperature of water. When the plenum length decreases, that is with increase in plenum aspect ratio, the heat transport from the wall decreases because of the entrance and exit conditions at the plenums. As the channel aspect ratio is increased to 7.57, the values of Nusselt numbers are more than doubled compared to the values observed for AR_c = 4.72 and the maximum Nusselt number is observed for U-type flow arrangement at AR_p = 2.5 as observed in the previous cases. This is because, reduced channel width and increased plenum length has favored the development of high wall shear stress resulting in high fluid momentum transport and the high heat intensity at this favorable flow conditions has resulted in enhanced heat transport from the wall to the bulk of the fluid, resulting in increased convective heat transfer. However, the rate of increase of Nusselt

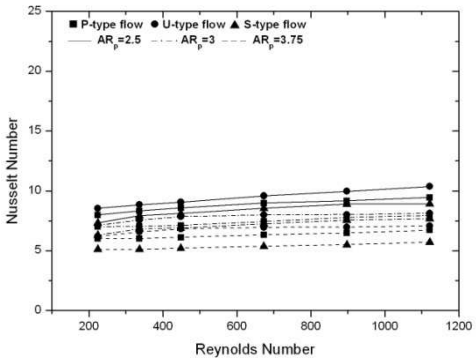

(a) AR_c = 4.72

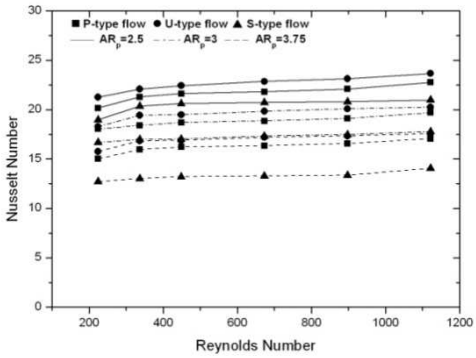

(b) AR_c = 7.57

Fig. 7. Effect of channel aspect ratio on Nusselt number at 375 W heat input.

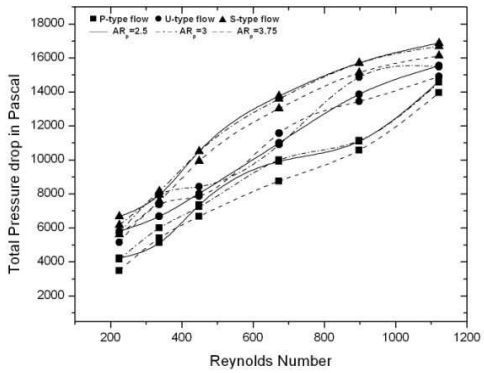

(a) AR_c = 4.72

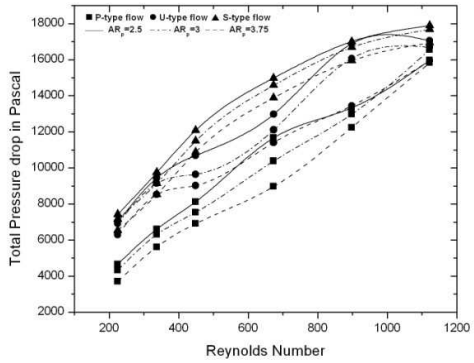

(b) AR_c = 7.57

Fig. 8. Effect of plenum aspect ratio on Nusselt number at 125 W.

numbers with Reynolds number is not pronounced as noted for the case of AR_c = 4.72. At this stage the flow field and thermal conditions might have been well established to achieve the maximum convective heat transfer. At higher value of channel aspect ratio, the plenum aspect ratio has significant effect for 375 W heat input.

3.4 Pressure drop variation within MCHS

The total pressure drop between the inlet and outlet plenum are obtained for all the test cases and are plotted as a function of Reynolds number, channel aspect ratio, plenum aspect ratio and flow arrangements for three heat inputs. Fig. 8(a) and 8(b) show the total pressure drop for AR_c = 4.72 and 7.57 respectively for three values of AR_p and three flow arrangements at 125 W heat input. The maximum pressure drop is observed for higher channel aspect ratio, AR_c = 7.57 and lowest plenum aspect ratio, AR_p = 2.5 for S-type flow arrangement, whereas the minimum pressure drop is noted for the case of P-type flow arrangement for AR_p = 3.75.

As the channel aspect ratio is increased, the fluid velocity through the channels also increases from 0.26 m/s to 0.38 m/s for the lowest Reynolds number 224.3 and from 1.28 m/s to 1.92 m/s for the highest Reynolds number 1121.7. The wall shear stress within the microchannels increases with increase in fluid velocity, resulting in higher pressure drop. The situation is different with plenum aspect ratio, wherein the pressure drop is found to be higher only for the lowest value of plenum aspect ratio. It is observed that the fluid flow travel length at the inlet/outlet plenum of the heat sink decreases with increase in plenum aspect ratio. Hence when the flow length is larger for the case of AR_p = 2.5, the pressure drop is found to be maximum. When the flow arrangements are considered, the S-type flow arrangement involves slightly longer flow path with two bends and hence gives rise to higher pressure drop compared to the P- and U-type flow arrangements.

In all the cases there is a continuous rise in the pressure drop with increase in Reynolds number as expected. For both the channel aspect ratios the U-type flow arrangement with AR_p = 2.5 that has given the maximum Nusselt number, takes a middle region of pressure drop as seen from the above figures. For the heat input of 225 W the total pressure drop are shown in Fig. 9(a) and 9(b) for AR_c = 4.72 and 7.57 respectively. Here again the maximum pressure drop seems to take place for S-type flow arrangement for AR_p = 2.5 for both the channel aspect ratios. However, all the pressure drop curves get clustered in two bunches with P-type flow arrangement occupying the lower pressure drop regions. The P-type and U-type flow arrangements at AR_p = 2.5 give rise to a non-uniform pressure variation with Reynolds number.

Fig. 10(a) and 10(b) show the pressure drop variation with Reynolds number for 375 W heat input for AR_c = 4.72 and

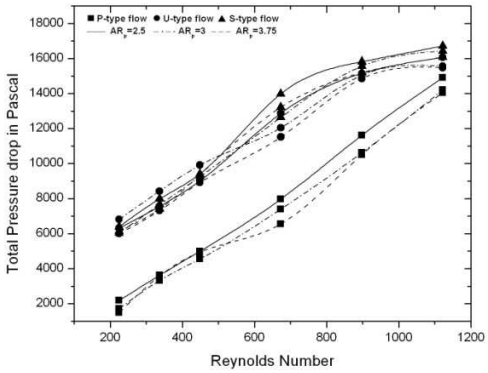

(a) AR_c = 4.72

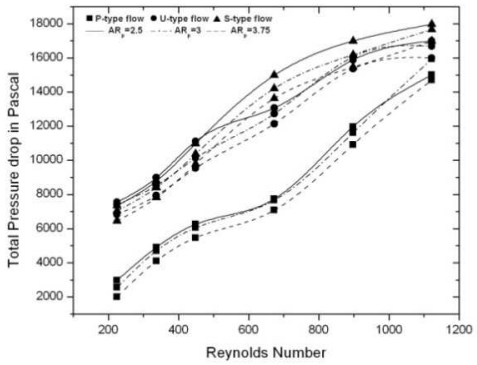

(b) AR_c = 7.57

Fig. 9. Effect of plenum aspect ratio on Nusselt number at 225 W.

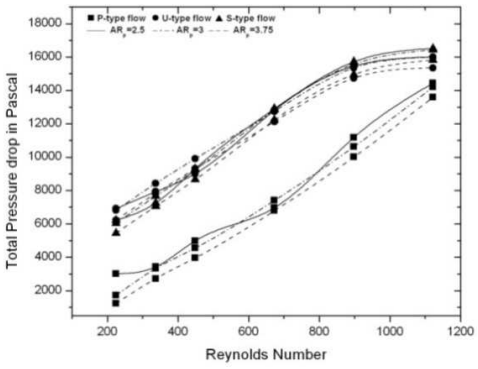

(a) AR_c = 4.72

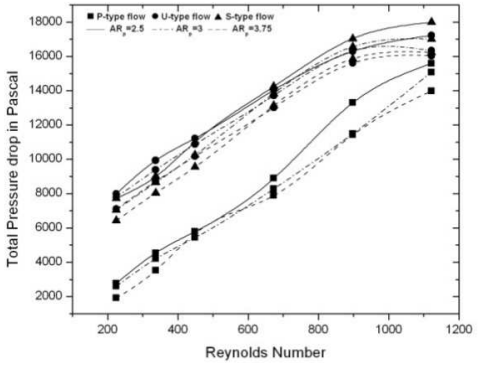

(b) AR_c = 7.57

Fig. 10. Effect of plenum aspect ratio on Nusselt number at 375 W.

7.57 respectively. It is seen from the above figures that the pressure drop increase with Reynolds number is more uniform compared to the cases shown in Figs. 8 and 9, except for a slight deviation observed at AR_c = 7.57, AR_p = 2.5 for P-type flow arrangement. Comparing Figs. 8, 9 and 10 one can easily notice that as the heat input increases from 125 W to 375 W, the lowest pressure drop obtained for P-type flow arrangement at AR_p = 3.75 decreases. The reason may be that with increased heat input the temperature of the fluid stream increases, which will result in slight decrease in viscosity of water used as coolant in the MCHS. In addition to this, increased heat input has increased the pressure drop difference observed between the P-type arrangement and the other two types of flow arrangements. The above figures indicate that for AR_c = 4.72 at 375 W heat input, the effect of plenum aspect ratio does not have significant effect on the pressure drop as compared to the variation in the pressure drop observed for 125 W heat input.

4. Conclusions

Experimental investigations have been carried out to examine the effect of channel and plenum aspect ratios at different flow arrangements on convective heat transfer and pressure drop characteristics of MCHS for various Reynolds number at different heat inputs. For this purpose three flow arrangements, P-, U- and S-types have been studied with three heat inputs. The data obtained from a detailed experimental study has been used to compute Nusselt number as a function of Reynolds number. Based on the analysis of the results the following conclusions can be drawn:

- The Nusselt number was seen to increase with increase in Reynolds number as expected and this rate of increase is not significantly affected by the variation in channel aspect ratio, plenum aspect ratio and flow arrangement except a small variation observed for AR_c = 7.57 at 125 W for the Reynolds number range 350 and 450.
- The Nusselt number was observed to increase by about 126 to 165% when the channel aspect ratio was increased from 4.72 to 7.57 (60.38%) due to increase in fluid velocity from the range 0.26 to 1.28 m/s to 0.38 to 1.92, giving rise to effective convective heat transfer and this trend has been observed almost for all the plenum aspect ratios.
- An increase about 18 to 26% in Nusselt number was noted when the plenum aspect ratio was reduced from 3.0 to 2.5 and about the same increase was noted when it was reduced from 3.75 to 3.0. However, the variation in Nusselt number was higher when the channel aspect ratio was increased to 7.57 and with increased heat input.
- As far as the flow arrangement is concerned the Nusselt number for U-type flow arrangement was found to be maximum 13% higher than the P-type and 10 to 27%

higher than the S-type for any given channel aspect ratio, plenum aspect ratio and heat input.

- For a given range of Reynolds number, the total pressure drop is observed maximum for S-type flow arrangement followed by U-type and P-type. With increase in plenum aspect ratio there is a decrease in the pressure drop with minimum pressure drop being experienced by P-type flow arrangement followed by U-type and S-type flow arrangements.

Nomenclature

A	: Area of channel (m^2)
AR	: Aspect ratio (dimensionless)
C	: Specific heat capacity (J/kgK)
Dc	: Depth of channel (m)
Dh	: Hydraulic diameter (m)
h	: Heat transfer coefficient (W/m^2K)
k	: Thermal conductivity (W/mK)
L	: Area of channel (m^2)
m	: Mass flow rate (kg/s)
N	: Number of microchannels
Nu	: Nusselt number (dimensionless)
P	: Pressure (bar)
q	: Heat (watt)
Q	: Volumetric flow rate (m^3/s)
Re	: Reynolds number (dimensionless)
T	: Temperature (K)
V	: Velocity (m/s)
W	: Width of channel (m)
x	: Horizontal distance (m)
y	: Vertical distance (m)

Greek symbols

ρ	: Density (kg/m^3)
μ	: Dynamic viscosity (Ns/m^2)

Subscripts & superscripts

c	: Channel
cu	: Copper
f	: Fluid
i	: Inlet
m	: Mean
o	: Outlet/exit
p	: Plenum

References

[1] D. B. Tuckerman and R. F. Pease, High-performance heat sinking for VLSI, *IEEE Electron Devices Letters*, EDL-2 (1981) 126-129.

[2] Kandlikar, Garimella, Li, Colin and King, *Heat transfer and fluid flow in minichannels and microchannels,* Elsevier Science, Great Britain, UK (2005).

[3] R. Chein and J. Chen, Numerical study of the inlet/outlet arrangement effect on microchannel heat sink performance, *International Journal of Thermal Sciences,* 48 (2009) 1627-1638.

[4] P. S. Lee and Suresh V. Garimella, Thermally developing flow and heat transfer in rectangular microchannels of different aspect ratios, *International Journal of Heat and Mass Transfer,* 49 (2006) 3060-3067.

[5] S. Jayaraj, S. Kang and Y. K. Suh, A review on the analysis and experiment of fluid flow and mixing in microchannels, *Journal of Mechanical Science and Technology,* 21 (3) (2007) 536-548.

[6] S. S. Sehgal, K. Murugesan and S. K. Mohapatra, Experimental investigation of the effect of flow arrangements on the performance of a microchannel heat sink, *Experimental Heat Transfer,* 24 (3) (2011) 215-233.

[7] P. S. Lee, Suresh V Garimella and D. Liu, Investigation of heat transfer in rectangular microchannels, *International Journal of Heat and Mass Transfer,* 48 (2005) 1688-1704.

[8] A. Kew Peter and A. Reay David, Compact/micro-heat exchangers their role in heat pumping equipment, *Applied Thermal Engineering,* 31 (2011) 594-601.

[9] D.-K. Kim and S. J. Kim, Closed-form correlations for thermal optimization of microchannels, *International Journal of Heat and Mass Transfer,* 50 (2007) 5318-5322.

[10] M. J. Kohl, S. I. Abdel-Khalik, S. M. Jeter and D. L. Sadowski, An experimental investigation of microchannel flow with internal pressure measurements, *International Journal of Heat and Mass Transfer* 48 (2005) 1518-1533.

[11] P. Kulkarni Devdatta and K. Das Debendra, Analytical and numerical studies on microscale heat sinks for electronic applications, *Applied Thermal Engineering* 25 (2005) 2432-2449.

[12] H.-C. Chiu, J.-H. Jang, H.-W. Yeh and M.-S. Wu, The heat transfer characteristics of liquid cooling heat sink containing microchannels, *International Journal of Heat and Mass Transfer,* 54 (2011) 34-42.

[13] G. Wang, P. Cheng and A. E. Bergles, Effects of inlet/outlet configurations on flow boiling instability in parallel microchannels, *International Journal of Heat and Mass Transfer,* 51 (2008) 2267-2281.

[14] L. Dorin, Effects of inlet geometry on heat transfer and fluid flow of tangential micro-heat sink, *International Journal of Heat and Mass Transfer,* 53 (2010) 3562-3569.

Satbir Singh Sehgal is faculty in Department of Mechanical & Automotive Engineering, Swift Institute of Engineering & Technology, Rajpura, India. He is M.Tech in Thermal Engineering from IIT Roorkee, India and is a part time research scholar in Department of Mechanical Engineering at Thapar University, Patiala, India. His research interests include experimental heat transfer, computational fluid dynamics and electronic cooling.

Krishnan Murugesan is an Assistant Professor in Department of Mechanical & Industrial Engineering, IIT Roorkee, India. He obtained his MTech and PhD degrees from IIT Bombay, Mumbai and IIT Madras, Chennai respectively. He worked as a Post-doctoral research fellow at Department of Civil Engineering, National Taiwan University, Taipei, Taiwan. He is in active research collaboration with Geoenvironmental Research Centre, Cardiff University, Cardiff, UK.

Saroj Kumar Mohapatra is Senior Professor in Department of Mechanical Engineering and Dean of Academic Affairs at Thapar University, Patiala, India. He is Ph.D and M.Tech from Indian School of Mines, India. He has guided number of PhDs and research projects of MHRD, DST, AICTE and UGC, India.